

Downlink CCM Estimation via Representation Learning with Graph Regularization

Melih Can Zerin, Elif Vural and Ali Özgür Yılmaz

Abstract—In this paper, we propose an algorithm for downlink (DL) channel covariance matrix (CCM) estimation for frequency division duplexing (FDD) massive multiple-input multiple-output (MIMO) communication systems with base station (BS) possessing a uniform linear array (ULA) antenna structure. We make use of the inherent similarity between the uplink (UL) CCM and the DL CCM due to angular reciprocity. We consider a setting where the UL CCM is mapped to DL CCM by a mapping function. We first present a theoretical error analysis of learning a nonlinear embedding by constructing a mapping function, which points to the importance of the Lipschitz regularity of the mapping function for achieving high estimation performance. Then, based on the theoretical ground, we propose a representation learning algorithm as a solution for the estimation problem, where Gaussian RBF kernel interpolators are chosen to map UL CCMs to their DL counterparts. The proposed algorithm is based on the optimization of an objective function that fits a regression model between the DL CCM and UL CCM samples in the training dataset and preserves the local geometric structure of the data in the UL CCM space, while explicitly regulating the Lipschitz continuity of the mapping function in light of our theoretical findings. The proposed algorithm surpasses benchmark methods in terms of three error metrics as shown by simulations.

Index Terms—Channel covariance matrix, massive MIMO, frequency division duplexing (FDD), Gaussian RBF interpolation, representation learning

I. INTRODUCTION

MASSIVE MIMO is a favorable technology for 5G and beyond networks in terms of achieving high spectral efficiency and energy efficiency [1]. In this technology, the base station (BS) has a high number of antennas, which is much more than the number of active user terminals [2]. However, there is a drawback of this technology for FDD systems: the excessive impractical pilot and feedback overhead [3], [4]. Since the uplink and downlink channels are not reciprocal in FDD systems, the channel estimation process consumes too much resource for pilot and feedback symbols due to the high number of antennas at the base station [3].

Cellular systems operate in time division duplexing (TDD) mode or frequency division duplexing (FDD) mode. Sharing the same wireless medium and frequency band, uplink and downlink channels are said to be reciprocal in TDD systems

The work of M. C. Zerin was supported by Turkcell Technology under 5G and Beyond Joint Graduate Support Program run by the Information and Communication Technologies Authority of Türkiye.

M. C. Zerin, E. Vural and A. Ö. Yılmaz are with the Department of Electrical and Electronics Engineering, Middle East Technical University, Ankara, Türkiye (e-mail: melih.zerin@metu.edu.tr, velif@metu.edu.tr, aoyilmaz@metu.edu.tr).

This work has been submitted to the IEEE for possible publication. Copyright may be transferred without notice, after which this version may no longer be accessible.

[5], which means that learning the uplink channel state information (CSI), the base station can infer the downlink CSI as well, and does not require any additional pilot training for downlink channel estimation. However, the reciprocity of uplink and downlink channels does not hold for FDD systems, because even though they share the same wireless medium, they operate using different carrier frequencies [6]. Thus, one cannot learn the DL CSI from its uplink counterpart in FDD systems, which is a huge disadvantage for the implementation of massive MIMO in these systems. As the number of base station antennas increases, the dimension of the downlink channel to be estimated also increases. Therefore, one needs to send more pilot signals to the users and receive feedback from them, in order to learn the DL CSI.

One solution to loosen the pilot and feedback overhead is to use the DL CCM instead of the DL CSI [4]. The channel covariance matrix provides a second order channel statistics, which may be useful for channel estimation and beamforming [7]. Therefore, it is an important parameter to know for the implementation of massive MIMO in FDD systems and knowing it as accurately as possible is highly important. In literature, there are numerous studies where the DL CCM is estimated by using the UL CCM, as in [8]–[14]. The motivation behind this choice is the following: Even though there is no channel reciprocity between the uplink and downlink channels, there is spatial reciprocity between them [15]. Therefore, their power distribution in the angular domain, i.e., their power angular spectrum (PAS), is commonly taken as the same. Thus, one can say that the UL CCM is quite informative about the DL CCM. Many of the fundamental approaches for the solution of this problem benefits from this property.

Some of the earlier works propose simple signal processing methods for the DL CCM estimation problem, such as [8], [9], [14]. On the other hand, much more complex tools like deep learning can also be incorporated into the solution of the UL-to-DL CCM transformation problem, as in [13]. Signal processing-based methods may experience performance degradation in practical cases where the UL CCM is not perfectly known. Their performance heavily depends on the availability of an accurate UL CCM and error propagation may occur in the cases where these methods are used to predict the DL CCM from noisy UL CCM estimates. Deep learning solutions are more robust to noise compared to classical methods due to the process of learning from the data. Nonetheless, in order to learn an accurate deep learning model with good generalization ability, one needs to use excessive amounts of data. Especially, as the number of base station antennas

increases, the size of the matrix to be learned will increase, which increases the need for more training data.

In this paper, for the DL CCM estimation problem, we propose to learn a nonlinear interpolation function which maps an arbitrary user's UL CCM to its DL CCM. In view of the above discussions, our idea is to seek a trade-off between simple signal processing-based methods and the complex deep learning solutions. We thus propose to learn a nonlinear interpolator that possesses the rich representation power of nonlinear methods with successful generalization capabilities, while involving fewer parameters to be optimized compared to neural networks in order to require much less training data. To the best of our knowledge, the estimation of DL CCMs from their UL counterparts via nonlinear interpolators has not yet been studied thoroughly in the current literature, due to which we aim to address both the theoretical and methodological aspects of this problem.

Inspired by the nonlinear supervised manifold learning approach in [16] that pays particular attention to the generalization of the learned embedding to previously unseen data, in this paper, we propose to solve the DL CCM estimation problem with representation learning with graph regularization. In [16], the authors give a theoretical performance analysis of a classification algorithm that jointly learns an embedding and an interpolation function that generalizes the embedding to previously unseen data. Although the method in [16] addresses a quite different application, i.e., data classification, some of the findings in [16] provide useful insights for the regression problem we consider in this paper. In particular, the principle of the preservation of the local geometry, which is employed in [10] as well, suggests that making the neighborhood relations between the points in the UL CCM space match those in the DL CCM space may have a positive impact on the estimation performance.

We first present a detailed theoretical analysis in order to explore the effect of the preservation of local geometry in the context of our regression problem along with the impact of the properties of the interpolation function used. Our theoretical results show that we should learn an embedding for DL CCMs from UL CCMs considering the following properties: (1) The local neighborhoods of the points in the UL CCM space should be preserved in the DL CCM space. (2) The embeddings of the UL CCMs in the training dataset should be close to the corresponding ground truth DL CCMs. (3) The interpolation function that maps UL CCMs to DL CCM estimates should have a low Lipschitz constant so that the function generalizes successfully to new UL CCMs that were not available during training.

Next, in the light of our theoretical findings, we propose an objective function, where a term related to the preservation of the local neighborhood structure and two terms related to the Lipschitz constant of the interpolator are optimized together with a data fitting term. We choose Gaussian RBF kernels for our interpolator, which provides a smooth interpolation of training data points by preventing sudden changes in the embedding space, i.e., overfitting, thanks to the Lipschitz regularity of the Gaussian kernel. We use an alternating optimization method to minimize the objective function in an

iterative fashion, in order to jointly learn the embedding and the parameters of the RBF interpolation function.

In this paper, our main contributions to the field of DL CCM estimation from UL CCM are the following:

- We first present a theoretical analysis of learning interpolation functions that map UL CCMs to their DL counterparts, with the purpose of identifying the main factors that affect the estimation error of the DL CCM. Our analysis shows that the error is essentially influenced by: (i) the average estimation error of the nearest neighbors of the point in the training dataset, (ii) the Lipschitz constant of the interpolation function, and (iii) the maximum value of the ratio of the distance between two DL CCMs to the distance between their UL counterparts.
- We next propose a novel representation learning method for DL CCM estimation, which builds on our theoretical results and relies on a model with much fewer parameters compared to other methods such as deep-learning based ones. The proposed method thus achieves considerably higher estimation performance in settings with limited availability of training data. Meanwhile, the nonlinear structure of the learnt model allows for successfully capturing the particular geometry of the data, making it favorable against simpler solutions such as linear transformations.

The paper is organized as follows: Section II summarizes the significant earlier works in the literature for the UL-DL CCM conversion problem. In Section III, the system model for the communication scenario is explained. In Section IV, the theoretical motivation behind our method is presented. A representation learning method for the problem of DL CCM estimation from UL CCMs is proposed in Section V. In Section VI, the performance of the proposed algorithm is compared to benchmark methods via simulations in terms of several error metrics, and a stability and sensitivity analysis is presented for the proposed algorithm. Finally, the concluding remarks are given in Section VII.

A bold lower case letter such as \mathbf{a} denotes a vector, while a bold upper case letter as in \mathbf{A} denotes a matrix. If \mathbf{A} is a square matrix, \mathbf{A}^{-1} and $tr(\mathbf{A})$ denote the inverse and the trace of \mathbf{A} , respectively. $(\cdot)^T$ and $(\cdot)^H$ denote transpose and Hermitian operators, respectively.

II. RELATED WORK

There are several creative solutions that try to estimate the DL channel state information (CSI) in an efficient way such as [17], [18], or to design feedback signals in an efficient manner as in [19]–[21]. In [22], a joint user grouping, scheduling and precoding design is developed based on CCMs of users in a multi-user environment. In [23], a joint pilot, feedback and precoder design is developed as a solution to the problematic FDD massive MIMO implementation issue. In [24], authors design an algorithm to find a pilot weighting matrix to shrink the feasible set of DL CCMs and find the center of the set in an FDD massive MIMO system with limited feedback and Type I codebook. In [25], a neural network architecture is trained for DL CSI estimation and DL beamforming by extracting

the joint long term properties of a wireless channel that is shared by both the UL and the DL channels due to the 'partial reciprocity' of UL/DL channels.

As the DL CSI estimation problem, DL CCM estimation is also a well-studied problem with numerous solutions proposed in the literature. In [8], a frequency calibration matrix is suggested to convert the UL CCM to its DL counterpart by taking the carrier frequency gap between UL and DL into account. In [9], a cubic splines method is suggested to interpolate the magnitude and the phase of DL CCM's elements from the corresponding UL CCM's elements. In [10], a dictionary is formed from UL/DL CCM pairs. When the DL CCM is to be estimated at an arbitrary point, its UL CCM is first represented as a weighted average of the UL CCMs in the dictionary, and then the same weights are used to interpolate the DL CCM from the DL CCMs in the dictionary.

There are several works in the literature that explicitly exploit the angular reciprocity concept by estimating the PAS from the UL CCM and using this estimate to form the corresponding DL CCM. [7], [11], [12] and [26] suggest methods to estimate the DL CCM in this manner, where the PAS is discretized for the estimation process. In [7], [11], the power distribution is estimated at certain angles, which corresponds to taking samples of the PAS in certain angles. In [12] and [26], the UL CCM is expressed by a system of equations, from which a discrete PAS is estimated. Then, the PAS estimation is used to find the DL CCM of the corresponding UL CCM.

On the other hand, using UL CCM to directly estimate DL CCM without explicitly finding the PAS is also an option, which is studied in several works such as [8], [10], [13], [14]. The method in [10] suggests using a dictionary of UL/DL CCM pairs for deduction of a new user's DL CCM with the help of its UL CCM and the dictionary created. A conditional generative adversarial networks (CGAN)-based method in [13] uses the image-to-image translation approach proposed in [27] by converting UL CCMs and DL CCMs into RGB images. In [14], the elements of UL CCM are considered as a non-linear transformed version of the common PAS of the UL and DL channels. Based on this property, a linear transformation method is proposed that maps an UL CCM to its DL CCM.

In this paper, the direct approach is followed without finding a PAS estimate explicitly. In literature, the machine learning-based studies that address the UL-to-DL CCM mapping problem generally use deep neural networks for this task. Although deep learning methods are able to learn highly complicated functions, they require tremendous amount of data for successful generalization, in contrast to simpler nonlinear interpolator structures with fewer parameters as chosen in our work.

III. SYSTEM MODEL

We consider an FDD single cell massive MIMO system, in which a base station (BS) containing M antennas forming a uniform linear array (ULA) serves single-antenna user equipments (UE). The UL channel operates at the carrier frequency of f_{ul} , and the DL channel operates at the carrier frequency of f_{dl} . Their respective wavelengths are denoted as λ_{ul} and λ_{dl} .

The ratio of carrier frequencies is denoted by $f_r = \frac{f_{dl}}{f_{ul}} = \frac{\lambda_{ul}}{\lambda_{dl}}$. UL and DL channels are considered to be frequency-flat.

We consider the wide sense stationary uncorrelated scattering (WSSUS) model for our communication scenario as in [14]. In this model, the autocorrelation function (acf) of the channel gain is time-invariant, and scattering at different angle of arrivals (AoA's) are uncorrelated. The ULA antenna structure and the WSSUS model lead CCMs to be Toeplitz. CCMs can then be formulated as [14]:

$$\mathbf{R}_x = \int_{\bar{v}-\Delta}^{\bar{v}+\Delta} p(\phi) \mathbf{a}_x(\phi) \mathbf{a}_x^H(\phi) d\phi \quad (1)$$

where $p(\phi)$ is the power angular spectrum (PAS), Δ is the spread of angle of arrivals (AoAs), \bar{v} is the mean AoA, $\mathbf{a}_x(\phi)$ is the array response vector at the angle ϕ , for $x \in \{UL, DL\}$. The array response vector is given by:

$$\mathbf{a}_x(\phi) = [1 \ e^{j2\pi \frac{d}{\lambda_x} \sin \phi} \ \dots \ e^{j2\pi \frac{d}{\lambda_x} (M-1) \sin \phi}]^T, \quad x \in \{UL, DL\}, \quad (2)$$

where $d = \frac{\lambda_{ul}}{2}$. The PAS is the same for uplink and downlink, and

it is normalized to 1, i.e., $\int_{\bar{v}-\Delta}^{\bar{v}+\Delta} p(\phi) d\phi = 1$. From (1) and (2), one can conclude that CCMs are Hermitian, i.e., $\mathbf{R}_x = \mathbf{R}_x^H$, for $x \in \{UL, DL\}$. Due to its Toeplitz structure, the \mathbf{R}_x matrix given in (1) can be represented by its first row.

IV. PERFORMANCE BOUNDS FOR DL CCM ESTIMATION VIA GAUSSIAN RBF KERNELS

In this section, first, the representation learning setting considered for the problem of DL CCM estimation from UL CCM is presented. Then, an upper bound on the error of an arbitrary test sample is provided.

A. Notation and Setting

Let $\{\mathbf{r}_{UL}^i, \mathbf{r}_{DL}^i\}_{i=1}^N$ be a training dataset with N training UL/DL CCM sample pairs, where $\mathbf{r}_x^i \in \mathbb{R}^{1 \times 2M-1}$ is a row vector obtained by the concatenation of the real and imaginary parts of the first row vector of the i^{th} CCM in the training dataset for $x \in \{UL, DL\}$. The first element of the first row of a CCM is always real, so it has no imaginary part. Hence, the vectors in the dataset are of length $2M-1$. Let the UL data samples be drawn i.i.d. from a probability measure ν on $\mathbb{R}^{1 \times 2M-1}$. The training samples are embedded into $\mathbb{R}^{1 \times 2M-1}$ such that each training sample \mathbf{r}_{UL}^i is mapped to a vector $\hat{\mathbf{r}}_{DL}^i \in \mathbb{R}^{1 \times 2M-1}$. The mapping is assumed to be extended to the whole data space through an interpolation function $f: \mathbb{R}^{1 \times 2M-1} \rightarrow \mathbb{R}^{1 \times 2M-1}$ such that each training sample is mapped to its embedding as $f(\mathbf{r}_{UL}^i) = \hat{\mathbf{r}}_{DL}^i$. Let \mathbf{r}_{UL}^{test} be the concatenated vector of an arbitrary UL CCM test point and $B_\delta(\mathbf{r}_{UL}^{test})$ be an open ball of radius δ around it:

$$B_\delta(\mathbf{r}_{UL}^{test}) := \{\mathbf{r}_{UL} \in \mathbb{R}^{2M-1} : \|\mathbf{r}_{UL}^{test} - \mathbf{r}_{UL}\| < \delta\}. \quad (3)$$

Let A^{UL} be the set of the training samples within a δ -neighborhood of \mathbf{r}_{UL}^{test} in $\mathbb{R}^{1 \times 2M-1}$

$$A^{UL} := \{\mathbf{r}_{UL}^i : \mathbf{r}_{UL}^i \in B_\delta(\mathbf{r}_{UL}^{test})\}. \quad (4)$$

Denoting the support of the probability measure v as $\mathcal{M} \subset \mathbb{R}^{1 \times 2M-1}$, we define

$$\eta_\delta := \inf_{\mathbf{r}_{UL}^{test} \in \mathcal{M}} v(B_\delta(\mathbf{r}_{UL}^{test})) \quad (5)$$

which is a lower bound on the measure of the open ball $B_\delta(\mathbf{r}_{UL}^{test})$ around any test point.

B. Theoretical Analysis for Motivation Behind the Proposed Method

We now present a theoretical analysis of the regression problem of UL-to-DL CCM conversion via a mapping function $f(\cdot)$. We consider a setting with the following assumptions:

- 1) The function $f : \mathbb{R}^{1 \times 2M-1} \rightarrow \mathbb{R}^{1 \times 2M-1}$ is Lipschitz continuous with constant L ; i.e., for any $\mathbf{r}_1, \mathbf{r}_2 \in \mathbb{R}^{1 \times 2M-1}$, $\|f(\mathbf{r}_1) - f(\mathbf{r}_2)\| \leq L\|\mathbf{r}_1 - \mathbf{r}_2\|$.
- 2) The probability measure v has a bounded support $\mathcal{M} \subset \mathbb{R}^{1 \times 2M-1}$.
- 3) For any $\delta > 0$, the probability measure lower bound η_δ is strictly positive, i.e., $\eta_\delta > 0$.

We examine the relation between the local geometries of the UL CCM and the DL CCM spaces with the following lemma:

Lemma 1. *Let \mathbf{p}_{UL}^i and \mathbf{p}_{UL}^j be two different points in $\mathbb{R}^{1 \times 2M-1}$ drawn i.i.d. from v , and let \mathbf{p}_{DL}^i and \mathbf{p}_{DL}^j be their DL counterparts. If $\|\mathbf{p}_{UL}^i - \mathbf{p}_{UL}^j\| \leq 2\delta$, then, there exists a constant $K > 0$ such that $\|\mathbf{p}_{DL}^i - \mathbf{p}_{DL}^j\| \leq K\|\mathbf{p}_{UL}^i - \mathbf{p}_{UL}^j\| \leq 2K\delta$, under the following assumptions:*

- The PAS, $p(\phi)$, is uniform.
- δ is so small that two points in a δ ball of a test point, say point i and point j , have very close mean Angle of Arrival (AoA) values, i.e., $\bar{v}_i - \bar{v}_j \approx 0$.
- The spread of AoA, Δ , of each data point in the dataset is constant and the same.

Proof of Lemma 1 is given in Appendix A.

Remark 1. Motivated by Lemma 1, for the given special case where the PAS is uniform and the angular spread of each user in a dataset is the same, one can say that if two points are close to each other in the UL CCM space, they should be close to each other in the DL CCM space as well. In practice, the constant K takes values close to f_r in realistic settings. We demonstrate this with a numerical analysis in Appendix D. Overall, Lemma 1 provides useful insight for settings where a mapping function is to be learned between the spaces of UL CCMs and DL CCMs.

For a sufficiently large dataset, i.e., for a sufficiently high N value, the distance between a point in the dataset and its nearest neighbors becomes considerably small, so that one can think of the ball radius parameter δ as a small constant. In Theorem 1, we consider such a setting and provide an upper bound on the test error of the estimate of an arbitrary test point obtained via the interpolation function $f(\cdot)$.

Theorem 1. *Let the training sample set contain at least N training samples $\{\mathbf{r}_{UL}^i\}_{i=1}^N$ with $\mathbf{r}_{UL}^i \sim v$. Let \mathbf{r}_{UL}^{test} be a test sample drawn from v independently of the training samples. Assume that the interpolation function $f : \mathbb{R}^{1 \times 2M-1} \rightarrow$*

$\mathbb{R}^{1 \times 2M-1}$ is a Lipschitz continuous function with Lipschitz constant L . Let $\epsilon > 0$, $\frac{1}{N\eta_\delta} \leq a < 1$ and $\delta > 0$ be arbitrary constants. Then, for a dataset with users having uniform PAS ($p(\phi)$) with the same AS (Δ), for sufficiently large N , with probability at least

$$(1 - \exp(-2N((1-a)\eta_\delta)^2)) \left(1 - 2\sqrt{2M-1} \exp\left(-\frac{aN\eta_\delta\epsilon^2}{2L^2\delta^2}\right)\right) \quad (6)$$

the following inequality holds

$$\begin{aligned} & \|\mathbf{r}_{DL}^{test} - f(\mathbf{r}_{UL}^{test})\| \\ & \leq \frac{1}{|A^{UL}|} \sum_{i:\mathbf{r}_{UL}^i \in A^{UL}} \|\mathbf{r}_{DL}^i - f(\mathbf{r}_{UL}^i)\| \\ & \quad + (L+K)\delta + \sqrt{2M-1}\epsilon. \end{aligned} \quad (7)$$

The proof of Theorem 1 is given in Appendix B.

Remark 2. Fixing the probability parameters $\delta > 0$ and $\epsilon > 0$ to sufficiently small constant values, one can see that the probability expression given in (6) approaches 1 at an exponential rate, as $N \rightarrow \infty$. Thus, it can be concluded that as $N \rightarrow \infty$, with probability approaching 1, the difference between a test point's estimation error and the average estimation error of training points within the δ -neighborhood of the test point can be made as small as desired. (One can choose the δ parameter sufficiently close to 0, as $N \rightarrow \infty$.) From this result, one can conclude the following:

- The smaller the average estimation error of the training points in the δ -neighborhood of the test point can be made via the algorithm used to learn the $f(\cdot)$ function, the smaller the upper bound on the estimation error of the test point gets. This can be achieved by arranging the objective function of the algorithm accordingly.
- Learning a function $f(\cdot)$ with a low Lipschitz constant L leads to a faster decrease in the upper bound. This can also be achieved by proper adjustments in the objective function of the algorithm. In practice, our result puts forward the following trade-off between the Lipschitz constant L and the training error: While one may reduce the training error to arbitrarily small values by increasing the complexity of $f(\cdot)$, this may come at the cost of learning a too irregular function with high Lipschitz constant L . Consequently, this causes poor generalization to new test data. A better strategy is to seek a trade-off between the minimization of the training error and the regularity of the learned interpolator $f(\cdot)$.

V. DL CCM ESTIMATION

In this section, we propose a representation learning algorithm motivated by the theoretical analysis in the previous section for the problem of DL CCM estimation from UL CCM.

A. Problem Formulation

Let $\mathbf{X} = [(\mathbf{r}_{UL}^1)^T \dots (\mathbf{r}_{UL}^N)^T]^T \in \mathbb{R}^{N \times (2M-1)}$ be the input training data matrix. Let $\mathbf{Y} = [\mathbf{y}_1^T \dots \mathbf{y}_N^T]^T \in \mathbb{R}^{N \times (2M-1)}$

be the embedding matrix, where $\mathbf{y}_i = f(\mathbf{x}_i)$. Let $\mathbf{R}_{true} = [(\mathbf{r}_{DL}^1)^T \dots (\mathbf{r}_{DL}^N)^T]^T \in \mathbb{R}^{N \times (2M-1)}$ be the output training data matrix. \mathbf{R}_{true} is the DL counterpart of \mathbf{X} .

Our aim is to find a function $f(\cdot)$ that approximates the training data sufficiently well, i.e., $f(\mathbf{x}_i) = \mathbf{y}_i \approx \mathbf{r}_{true,i}$, and preserves the nearest neighbors of each input vector in the embedding space, while mapping previously unseen UL CCMs (test data) to DL CCMs with low error. The interpolation problem can be formulated considering the following objectives.

Lipschitz regularity of the interpolation function: The interpolation function is of the form

$$f(\mathbf{x}) = [f^{(1)}(\mathbf{x}) \ f^{(2)}(\mathbf{x}) \ \dots \ f^{(2M-1)}(\mathbf{x})]. \quad (8)$$

Here $f(\cdot)$ is chosen as a radial basis function (RBF) interpolator due to its well-studied properties [28]. Specifically, the Gaussian RBF kernel is chosen for the extension of the embedding, where

$$f^{(k)}(\mathbf{x}) = \sum_{i=1}^N C_{ik} e^{-\frac{\|\mathbf{x}-\mathbf{x}_i\|^2}{\sigma^2}} \quad (9)$$

is the k^{th} element of $f(\mathbf{x})$, for $k \in \{1, \dots, 2M-1\}$. C_{ik} are the interpolator coefficients, and σ is the scale parameter of the Gaussian RBF kernel.

The Lipschitz constant of the Gaussian RBF interpolation function is provided in [16] as

$$L = \sqrt{2}e^{-1/2}\sqrt{N}\sigma^{-1}\|\mathbf{C}\|_F, \quad (10)$$

where $\mathbf{C} \in \mathbb{R}^{N \times (2M-1)}$ is the matrix containing the interpolator coefficient C_{ik} in its $(i, k)^{th}$ element, $i \in \{1, \dots, N\}$, $k \in \{1, \dots, 2M-1\}$. The matrix \mathbf{C} is obtained as

$$\mathbf{C} = \Psi^{-1}\mathbf{Y}, \quad (11)$$

by learning a mapping \mathbf{Y} from the training data matrix \mathbf{X} , where $\Psi \in \mathbb{R}^{N \times N}$ is the RBF kernel matrix, whose $(i, j)^{th}$ element is $e^{-\frac{\|\mathbf{x}_i-\mathbf{x}_j\|^2}{\sigma^2}}$.

From Theorem 1, the Lipschitz constant, L , of the interpolator, $f(\cdot)$, should be small so as to reduce the error upper bound in (7), which leads to a good generalization of the embedding to the test data. With that in mind, according to (10), the following terms should be minimized while learning embedding coordinates and the function parameters of the RBF interpolator:

- σ^{-2}
- $\|\mathbf{C}\|_F^2 = \|\Psi^{-1}\mathbf{Y}\|_F^2 = tr(\mathbf{Y}^T\Psi^{-2}\mathbf{Y})$

Preservation of the local geometry between the UL/DL CCM spaces: Due to the angular reciprocity, there is an inherent similarity between the UL CCM and DL CCM of the same user, even though there is no explicit function that relates one another. On the other hand, from Lemma 1, one can see that with enough training data, the points in the UL space become so close that the distance between nearest neighbors is bounded proportionally to the distance between their corresponding points in the DL space. Therefore, in order

to preserve the local geometry of UL CCMs in the embedding space, the following term should be minimized

$$\sum_{i,j=1}^N (\mathbf{W})_{ij} \|\mathbf{y}_i - \mathbf{y}_j\|^2 = tr(\mathbf{Y}^T\mathbf{L}\mathbf{Y}), \quad (12)$$

where \mathbf{W} is a weight matrix whose $(i, j)^{th}$ entry is given by $(\mathbf{W})_{ij} = e^{-\frac{\|\mathbf{x}_i-\mathbf{x}_j\|^2}{\theta^2}}$ (for a scale parameter θ), $\mathbf{L} = \mathbf{D} - \mathbf{W}$ is the Laplacian matrix, and \mathbf{D} is the diagonal degree matrix with i^{th} diagonal entry $(\mathbf{D})_{ii} = \sum_j (\mathbf{W})_{ij}$. The weights in the weight matrix are selected according to the pairwise distances between data pairs, i.e., $\|\mathbf{x}_i - \mathbf{x}_j\|$ for $i, j \in \{1, \dots, N\}$, $i \neq j$. In this way, for nearby $(\mathbf{x}_i, \mathbf{x}_j)$ pairs with strong edge weights, a high penalty is applied to the action of mapping \mathbf{y}_i and \mathbf{y}_j far from one another, which preserves the structure of the local neighborhoods between the UL and the DL domains [29]. The equality in (12) is shown in [29].

UL/DL CCM pairs in the training dataset: Since the task is to learn a function that maps UL CCMs to their corresponding DL CCMs, the UL-DL CCM pairs in the training dataset are also incorporated into our optimization problem. Instead of employing hard data fidelity constraints, in order to achieve better noise tolerance we prefer the quadratic penalty term given by

$$\|\mathbf{Y} - \mathbf{R}_{true}\|_F^2.$$

Overall problem: We finally combine the above terms to form our overall objective function as

$$\min_{\mathbf{Y}, \sigma} tr(\mathbf{Y}^T\mathbf{L}\mathbf{Y}) + \mu_1 tr(\mathbf{Y}^T\Psi^{-2}\mathbf{Y}) + \mu_2\sigma^{-2} + \mu_3\|\mathbf{Y} - \mathbf{R}_{true}\|_F^2, \quad (13)$$

where μ_1 , μ_2 and μ_3 are positive weights to determine the relative importance of each term in the objective function.

B. Solution of the Problem

The optimization problem defined above is not jointly convex in \mathbf{Y} and σ . We employ an alternating optimization method, where one of the parameters is fixed while the other one is optimized in an alternative fashion at each iteration. This alternation is continued until convergence or the maximum number of iterations is reached.

Optimization of \mathbf{Y} : When σ is fixed, the optimization problem in (13) becomes the following:

$$\min_{\mathbf{Y}} tr(\mathbf{Y}^T\mathbf{L}\mathbf{Y}) + \mu_1 tr(\mathbf{Y}^T\Psi^{-2}\mathbf{Y}) + \mu_3\|\mathbf{Y} - \mathbf{R}_{true}\|_F^2 \quad (14)$$

This minimization problem is a quadratic and convex problem. The closed form solution of the problem in (14) is given by

$$\mathbf{Y}^* = \mu_3(\mathbf{A} + \mu_3\mathbf{I})^{-1}\mathbf{R}_{true}, \quad (15)$$

where $\mathbf{A} = \mathbf{L} + \mu_1\Psi^{-2}$. The eigenvalues of a graph Laplacian matrix are always nonnegative, i.e., the Laplacian matrix is a positive semidefinite matrix. Therefore, the $(\mathbf{A} + \mu_3\mathbf{I})$ is always invertible.

Optimization of σ : When \mathbf{Y} is fixed, the optimization problem is the following:

$$\min_{\sigma} \mu_1 \text{tr}(\mathbf{Y}^T \boldsymbol{\Psi}^{-2} \mathbf{Y}) + \mu_2 \sigma^{-2} \quad (16)$$

Although nonconvex, this problem involves the optimization of a single scalar variable σ , which can be solved via an exhaustive search of σ in a reasonable interval.

Our solution algorithm is summarized in Algorithm 1.

Algorithm 1: DL CCM Interpolation via Gaussian RBF Kernel

input : Training data matrices \mathbf{X} and \mathbf{R}_{true}

Initialization:

Construct the graph Laplacian matrix \mathbf{L} and the RBF kernel matrix $\boldsymbol{\Psi}$

Assign weight parameters μ_1 , μ_2 and μ_3 and initial values of σ and \mathbf{Y}

repeat

 Minimize \mathbf{Y} by fixing σ ;

 Minimize σ by fixing \mathbf{Y} ;

until convergence of the objective function or the maximum iteration number is reached;

output: Kernel scale parameter σ , embedding matrix \mathbf{Y}

After learning the embedding matrix \mathbf{Y} and the kernel scale parameter σ with Algorithm 1, one can calculate the interpolator coefficient matrix \mathbf{C} by using equation (11). Thus, using (8) and (9), one can estimate the DL CCM of a new test sample that is not in the training dataset by using its UL CCM.

The integral of PAS over all angles is known to be 1; however we have no constraints forcing such a normalization while learning the embedding and the kernel scale parameter. For this reason, once we obtain the estimate $\hat{\mathbf{r}}_{DL}$, we normalize it such that its first entry becomes $\hat{\mathbf{r}}_{DL}(1) = 1$.

C. Complexity Analysis

The main factors that determine the complexity of our algorithm are the optimization problems given in (14) and (16), which are solved in an alternating fashion. The complexity of constructing the matrices \mathbf{L} and $\boldsymbol{\Psi}$ is $\mathcal{O}(MN^2)$, where N is the number of training data in the dataset. The matrix inversion operations in (15) and (16) are of complexity $\mathcal{O}(N^3)$, which is the determining part of the complexity analysis, in a typical scenario where $M < N$. Hence, the overall complexity of our algorithm is $\mathcal{O}(N^3)$.

After the training is completed, the Gaussian RBF interpolation function can be directly used to find the DL CCMs of new data. The complexity of finding an estimate of the DL CCM using our function is $\mathcal{O}(M^2N)$ since for each element of the mapping vector of size $(2M - 1)$, $(2M - 1)$ -dimensional vectors are used for calculation at N center locations. [30].

VI. SIMULATIONS

In this section, we evaluate the performance of our algorithm with simulations, based on the simulation setup reported

in Table I. We first observe the behavior of the objective function and that of the estimation performance of our method throughout the iterations. Next, we conduct tests to study how the performance of our method varies with algorithm hyperparameters. Finally, we compare the performance of our method to that of some baseline methods in the literature.

TABLE I
SIMULATION PARAMETERS

Carrier Frequencies	$f_{UL} = 1.95$ GHz, $f_{DL} = 2.14$ GHz
Base Station Antenna Number (M)	One of the following: {32, 64, 128, 256}
Dataset Size (Train and Test)	500
Train/Test Data Ratio	80%/20%
μ_1, μ_2, μ_3	0.1, $3 \times 10^5, 100$
SNR	20 dB

Users are considered to have uniform PAS with mean AoAs uniformly distributed in $[-\pi, \pi]$. The spread of AoAs of users are drawn from $[5^\circ, 15^\circ]$ uniformly. The carrier frequencies of uplink and downlink channels in Table I are chosen according to [31].

Let us denote the true value of a DL CCM by \mathbf{R}_{DL} and its estimate by $\hat{\mathbf{R}}_{DL}$. The following three error metrics are used to compare the performance of the proposed algorithm with benchmark methods:

- 1) Normalized Mean Square Error (NMSE): NMSE is used to measure the average error in each entry of a CCM, which is defined as

$$\text{NMSE} = \mathbb{E} \left\{ \frac{\|\mathbf{R}_{DL} - \hat{\mathbf{R}}_{DL}\|_F^2}{\|\mathbf{R}_{DL}\|_F^2} \right\}. \quad (17)$$

- 2) Correlation Matrix Distance (CMD): This metric defined in [32] is used to quantify the deviation between the direction of the true DL CCM and that of its estimate. The CMD is given by

$$\text{CMD} = \mathbb{E} \left\{ 1 - \frac{\text{tr}(\mathbf{R}_{DL} \hat{\mathbf{R}}_{DL})}{\|\mathbf{R}_{DL}\|_F \|\hat{\mathbf{R}}_{DL}\|_F} \right\}. \quad (18)$$

- 3) Deviation Metric (DM): In [14], the following deviation metric is used to measure the deviation in the principal eigenvector of the estimated DL CCM, which is useful in beamforming applications:

$$\text{DM} = 1 - \frac{\text{tr}(\mathbf{v}^H \mathbf{R}_{DL} \mathbf{v})}{\Gamma_{max}}, \quad (19)$$

where Γ_{max} is the largest eigenvalue of \mathbf{R}_{DL} and \mathbf{v} is the eigenvector corresponding to the largest eigenvalue of $\hat{\mathbf{R}}_{DL}$.

A. Simulation Setup

The dataset is constructed similarly to the setting in [14] as described below. The following steps are followed for all UL CCMs in the dataset and for DL CCMs in the training dataset. DL CCMs in the test set are constructed via only Step 1, so that they form an ideal ground truth data set for performance comparisons of our algorithm with the benchmark methods.

- 1) CCMs are calculated using the formula in (1).
- 2) Using the generated CCMs, UL and DL channel realizations are constructed as follows:

$$\left(\mathbf{h}_x^k\right)^c = \left(\mathbf{R}_x^k\right)^{1/2} \left(\mathbf{w}_x^k\right)^c, c = 1, \dots, N_{ch},$$

$$x \in \{UL, DL\}, \quad (20)$$

where $\left(\mathbf{w}_x^k\right)^c \sim \mathcal{CN}(\mathbf{0}, \mathbf{I})$, \mathbf{R}_x^k is the CCM of user k (either UL or DL, specified by x) and N_{ch} is the number of channel realizations. N_{ch} is taken as $2M$ in the simulations.

- 3) The noisy channel estimates obtained after the training phase with pilot signals are modeled and generated as follows:

$$\left(\hat{\mathbf{h}}_x^k\right)^c = \left(\mathbf{h}_x^k\right)^c + \left(\mathbf{n}_x^k\right)^c, c = 1, \dots, N_{ch},$$

$$x \in \{UL, DL\} \quad (21)$$

where $\left(\mathbf{n}_x^k\right)^c \sim \mathcal{CN}(\mathbf{0}, \sigma^2 \mathbf{I})$ and $\left(\hat{\mathbf{h}}_x^k\right)^c$ is the noisy channel estimate of the c^{th} channel realization. The signal-to-noise ratio (SNR) for this pilot signaling setup is taken to be the same as in [14], which is $\frac{\text{tr}(\mathbf{R}_{UL}^k)}{\sigma^2} = 20$ dB, unless it is explicitly said to be taken differently.

- 4) The sample covariance for user k is then given by

$$\hat{\mathbf{R}}_x^k = \frac{1}{N_{ch}} \sum_{c=1}^{N_{ch}} \left(\hat{\mathbf{h}}_x^k\right)^c \left(\hat{\mathbf{h}}_x^k\right)^{cH} - \sigma^2 \mathbf{I},$$

$$x \in \{UL, DL\}. \quad (22)$$

- 5) Due to the ULA antenna structure at the BS and the WSSUS model, the CCMs are Toeplitz, Hermitian and PSD, which is used for the correction of the sample covariance found in (22). The projection of the sample covariance onto the set of Toeplitz, Hermitian and PSD matrices is done by the alternative projection method proposed in [33]. The projection method solves the following optimization problem:

$$\tilde{\mathbf{R}}_x^k = \arg \min_{\mathbf{X} \in T_+^M} \|\mathbf{X} - \hat{\mathbf{R}}_x^k\|^2 \quad (23)$$

where T_+^M is the set of $M \times M$ Toeplitz, Hermitian and PSD matrices.

- 6) The matrices estimated in the previous step are normalized so that their $(1, 1)^{th}$ element is 1. This is done due to the fact that the PAS of the CCMs are normalized to 1.

B. Stability and Sensitivity Analysis

First, we study the change in the objective function and the change in the average NMSE of DL CCMs learned by our algorithm throughout the iterations. For $M = 64$ base station antennas, we repeat the experiments for 25 i.i.d. datasets. The average objective function and error values are presented in Figure 1. From Figure 1, one can see that the objective function decreases throughout the iterations, which is expected because the algorithm updates both the embedding and the kernel scale parameter in such a way that the objective function

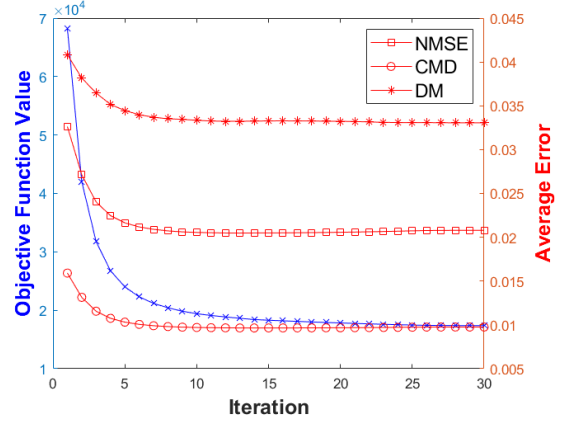


Fig. 1. The changes on the objective function and the average error performance throughout the iterations

never increases. The average NMSE, CMD and DM follow a similar trend to decrease as the objective function, which suggests that our proposed objective function well captures the performance goal of our algorithm.

Next, we conduct a sensitivity analysis in order to examine the effect of the hyperparameters (μ_1, μ_2, μ_3) on the performance of our algorithm. Tables II and III show the NMSE values of the DL CCM estimates of our algorithm for several (μ_1, μ_2, μ_3) combinations. For each (μ_1, μ_2, μ_3) , we repeat the experiments for 10 i.i.d. datasets, where the base station has $M = 64$ antennas. The average NMSE values are presented in Tables II and III. Table II shows the necessity of the Lipschitz constant-related terms, since the performance gets better as μ_1 and μ_2 increase together from 0 up to around $\mu_1 = 10^{-1}$ and $\mu_2 = 3 \times 10^5$. After that point, the performance gets worse, since the Lipschitz constant-related terms start to dominate the objective function in (13), which decreases the significance of the data fidelity terms in the objective function. This causes the mappings of the training points to deviate from their true values and eventually results in a performance degradation.

Table III reports the performance for different weight combinations for the Lipschitz continuity of the interpolator and the data fidelity. The ratio between μ_1 and μ_2 is fixed to a suitable number chosen based on Table II. Looking at Table III, one can see that as μ_3 gets smaller, the average NMSE increases drastically. However, it also shows that μ_1 (and also μ_2) should be chosen as positive numbers to improve the performance. The performance seems to be more sensitive to the data fidelity term than the Lipschitz continuity terms.

C. Algorithm Performance

In this section, we compare the average errors of our method to those of the following three benchmark methods: (1) The dictionary based method in [10], (2) the sinc transformation-based method in [14], (3) the CGAN-based method in [13]. We conduct three different experiments. First, we calculate the DL CCM estimation errors with a perfect dataset to study the performances of the compared methods. Then, we calculate the

TABLE II
THE VARIATION OF THE NMSE WITH THE HYPERPARAMETERS μ_1 AND μ_2 FOR FIXED $\mu_3 = 100$

$\mu_2 \backslash \mu_1$	0	10^{-4}	10^{-3}	10^{-2}	10^{-1}	1	10^1	10^2
0	0.0463	0.0390	0.0390	0.0389	0.0376	0.0345	0.0309	0.0402
3×10^{-1}	0.0463	0.0348	0.0378	0.0387	0.0376	0.0345	0.0309	0.0402
3×10^1	0.0463	0.0313	0.0320	0.0344	0.0361	0.0343	0.0309	0.0402
3×10^3	0.0463	0.0349	0.0325	0.0307	0.0297	0.0298	0.0300	0.0403
3×10^5	0.0463	0.0265	0.0221	0.0194	0.0201	0.0238	0.0319	0.0452
3×10^7	0.0463	0.0265	0.0221	0.0194	0.0208	0.0313	0.0540	0.0796
3×10^9	0.0463	0.0265	0.0221	0.0194	0.0208	0.0313	0.0540	0.1022
3×10^{11}	0.0463	0.0265	0.0221	0.0194	0.0208	0.0313	0.0540	0.1022

TABLE III
THE VARIATION OF THE NMSE WITH THE HYPERPARAMETERS μ_1 AND μ_3 FOR $\mu_2 = 3 \times 10^6 \mu_1$

$\mu_3 \backslash \mu_1$	0	10^{-4}	10^{-3}	10^{-2}	10^{-1}	1	10^1	10^2
10^{-1}	0.2093	0.2248	0.2448	0.2550	0.2739	0.3643	0.6225	0.8106
1	0.0722	0.0704	0.0682	0.0730	0.0858	0.1252	0.2766	0.6016
10^1	0.0357	0.0315	0.0277	0.0241	0.0347	0.0566	0.1043	0.2657
10^2	0.0463	0.0324	0.0325	0.0275	0.0201	0.0311	0.0540	0.1022
10^3	0.0496	0.0330	0.0331	0.0335	0.0283	0.0199	0.0308	0.0538
10^4	0.0500	0.0331	0.0331	0.0332	0.0336	0.0284	0.0198	0.0307
10^5	0.0500	0.0331	0.0331	0.0331	0.0332	0.0336	0.0284	0.0198

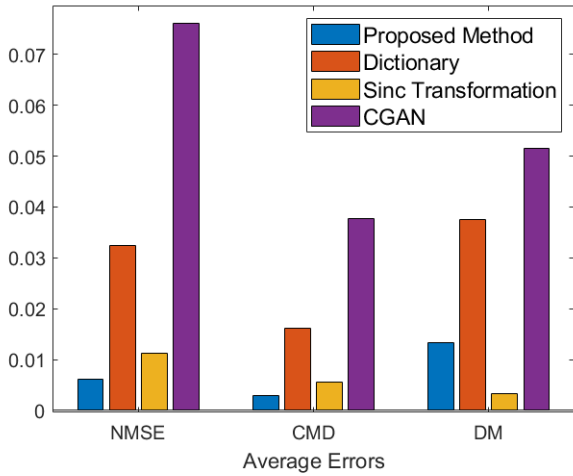


Fig. 2. Average error values for our method and the benchmark methods for a perfect dataset with CCMs of a $M = 256$ base station antenna system

DL CCM estimation errors for different SNR values. Finally, we compare the error values of the algorithms for different numbers of base station antennas, M .

In Figure 2, we compare the performances of all benchmark methods for $M = 256$ base station antennas where the CCMs in both the training and the test datasets are perfectly known. The results are averaged over 10 i.i.d. datasets. For this experiment, the hyperparameters are taken as $\mu_1 = 10$, $\mu_2 = 3 \times 10^8$ and $\mu_3 = 10^7$. One can see from Figure 2 that our algorithm mostly outperforms the dictionary based method and the sinc transformation method, while the CGAN-based method has relatively higher error values than the other methods. In particular, our method yields the smallest average NMSE value of 6.1×10^{-3} among all methods, while its closest competitor algorithms dictionary and sinc transformation methods result in average NMSE values of 0.0324 and 0.0112, respectively. On the other hand, the average NMSE of the CGAN based

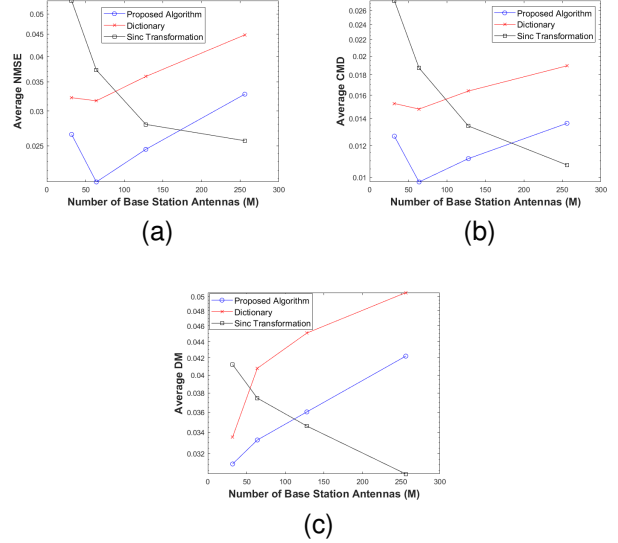


Fig. 3. The error performances of the algorithms against different base station antenna numbers for SNR = 20 dB (a) NMSE (b) CMD (c) DM

method for this setup is 0.0761. One can interpret this finding as follows: Even though deep learning based methods can learn highly complex functions quite well, they need a large amount of data to achieve this. In settings with a limited availability of training data, such methods may fail to learn a network that can generalize to new data well. Considering also the long training processes, in the rest of our experiments we compare our algorithm with the dictionary based method and the sinc transformation method, since they are closer to our method in terms of performance.

Figure 3 demonstrates the average error values of each algorithm for the base station antenna numbers of $M \in \{32, 64, 128, 256\}$. For 25 i.i.d. datasets, the experiments are repeated and the average errors are presented in Figure 3. One can see that the proposed algorithm surpasses the performance of dictionary-based method for each error metric for all antenna numbers. However, the sinc transformation method has better average error performance than our method for high number of antennas, for example $M = 256$ antennas. This result is expected, since the methods that rely on training data, i.e., the dictionary method and our algorithm, both try to estimate more matrix parameters with the same dataset size, which gets more difficult as the number of base station antennas increases. On the other hand, the sinc transformation method has an error upper bound that decreases with the antenna number, M , which is presented in [14]. Even though the average error of the sinc transformation method is lower than that of our method for $M = 256$ antennas, we have observed the standard deviations of the NMSE values for our method, dictionary method and the sinc transformation method to be 0.0161, 0.0377 and 0.0343, respectively. One can deduce from these results that even though our algorithm may yield higher average error than the sinc transformation method at a high number of antennas, its error performance is more stable than that of the sinc transformation method, i.e., it is less likely to encounter outliers with significantly high error values.

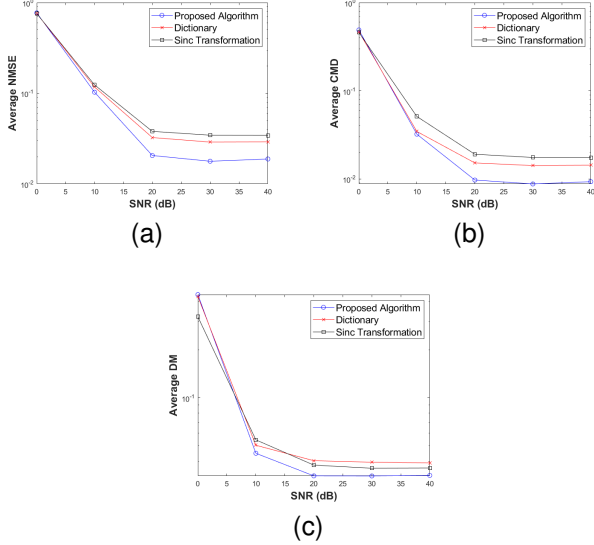


Fig. 4. The error performances of the algorithms against different SNR values when the base station antenna number is $M = 64$ (a) NMSE (b) CMD (c) DM

Figure 4 shows the performances of the algorithms when the base station has $M = 64$ antennas. The experiments are repeated for 25 i.i.d. datasets. In this scenario, the CCMs have been constructed for several different SNR values ranging from 0 dB to 40 dB and the effect of the SNR on the performance is observed. One can see that all algorithms yield high estimation error at 0 dB SNR as expected, where the CCMs are corrupted with severe noise. As the SNR increases, the estimates obtained from each algorithm improves and our algorithm outperforms the benchmark methods in all performance metrics.

VII. CONCLUSION

In this paper, we have proposed a novel DL CCM estimation method for FDD massive MIMO systems where the base station is equipped with ULA antennas. We have first presented a theoretical analysis that gives an upper bound on the estimation error of the DL CCM from UL CCMs. We have then proposed a representation learning-based method in order to learn a mapping function from UL CCMs to their DL CCM counterparts. The proposed method aims at learning an interpolation function from datasets relatively smaller than those needed for training deep neural networks, while capturing the richness of nonlinear learning methods so that the learned mapping is more robust to nonlinearities/discrepancies in the system parameters than simple signal processing based methods. The experimental results show that the proposed algorithm achieves better estimation performance than the benchmark methods in most of the scenarios. The proposed method can especially be useful in practical applications with limited access to training data. Our algorithm shows promising performance in such applications as it provides quite accurate downlink channel covariance estimates with a simple nonlinear learning setup. The extension of our method to other base station antenna

structures, such as a uniform rectangular array (URA) is left as a future research direction.

ACKNOWLEDGMENTS

The authors would like to thank Dr. -Ing. Bitan Banerjee for offering his help for the implementation of the CGAN-based benchmark method in [13].

APPENDIX A PROOF OF LEMMA 1

$$\begin{aligned}
 \|\mathbf{p}_{UL}^i - \mathbf{p}_{UL}^j\|^2 &= \sum_{m=1}^M \left| [\mathbf{p}_{UL}^i]_m - [\mathbf{p}_{UL}^j]_m \right|^2 \\
 &= \sum_{m=1}^M \left| \int_{\bar{v}_i - \Delta}^{\bar{v}_i + \Delta} p(\phi) \exp(j\pi(m-1)\sin(\phi)) d\phi \right. \\
 &\quad \left. - \int_{\bar{v}_j - \Delta}^{\bar{v}_j + \Delta} p(\phi) \exp(j\pi(m-1)\sin(\phi)) d\phi \right|^2 \\
 &= \sum_{m=1}^M \left| \int_{\bar{v}_i - \Delta}^{\bar{v}_i + \Delta} \frac{1}{2\Delta} \exp(j\pi(m-1)\sin(\phi)) d\phi \right. \\
 &\quad \left. - \int_{\bar{v}_j - \Delta}^{\bar{v}_j + \Delta} \frac{1}{2\Delta} \exp(j\pi(m-1)\sin(\phi)) d\phi \right|^2 \\
 &= \sum_{m=1}^M \left| \int_{\bar{v}_j + \Delta}^{\bar{v}_i + \Delta} \frac{1}{2\Delta} \exp(j\pi(m-1)\sin(\phi)) d\phi \right. \\
 &\quad \left. - \int_{\bar{v}_j - \Delta}^{\bar{v}_i - \Delta} \frac{1}{2\Delta} \exp(j\pi(m-1)\sin(\phi)) d\phi \right|^2 \quad (24)
 \end{aligned}$$

Let us define $\theta := \pi \sin(\phi)$. The limits of the integrals in Equation (24) cover very narrow intervals due to the condition $\bar{v}_i - \bar{v}_j \approx 0$ given in Lemma 1. Therefore, one can approximate θ as a linear function of ϕ in these intervals using a first order Taylor approximation.

For $\phi \in [\bar{v}_j + \Delta, \bar{v}_i + \Delta]$,

$$\begin{aligned}
 \sin(\phi) &\approx \sin\left(\frac{\bar{v}_i + \bar{v}_j}{2} + \Delta\right) \\
 &+ \left(\frac{\cos\left(\frac{\bar{v}_i + \bar{v}_j}{2} + \Delta\right)}{1!}\right) \left(\phi - \left(\frac{\bar{v}_i + \bar{v}_j}{2} + \Delta\right)\right). \quad (25)
 \end{aligned}$$

Therefore, one can approximate θ as $\theta \approx \alpha_1 \phi + \beta_1$, where

$$\alpha_1 = \pi \cos\left(\frac{\bar{v}_i + \bar{v}_j}{2} + \Delta\right) \quad (26)$$

and

$$\begin{aligned}
 \beta_1 &= \pi \left[\sin\left(\frac{\bar{v}_i + \bar{v}_j}{2} + \Delta\right) \right. \\
 &\quad \left. - \left(\frac{\bar{v}_i + \bar{v}_j}{2} + \Delta\right) \cos\left(\frac{\bar{v}_i + \bar{v}_j}{2} + \Delta\right) \right]. \quad (27)
 \end{aligned}$$

Similarly, for $\phi \in [\bar{v}_j - \Delta, \bar{v}_i - \Delta]$,

$$\begin{aligned} \sin(\phi) &\approx \sin\left(\frac{\bar{v}_i + \bar{v}_j}{2} - \Delta\right) \\ &+ \left(\frac{\cos\left(\frac{\bar{v}_i + \bar{v}_j}{2} - \Delta\right)}{1!}\right) \left(\phi - \left(\frac{\bar{v}_i + \bar{v}_j}{2} - \Delta\right)\right). \end{aligned} \quad (28)$$

Therefore, one can approximate θ as $\theta \approx \alpha_2\phi + \beta_2$, where

$$\alpha_2 = \pi \cos\left(\frac{\bar{v}_i + \bar{v}_j}{2} - \Delta\right) \quad (29)$$

and

$$\begin{aligned} \beta_2 &= \pi \left[\sin\left(\frac{\bar{v}_i + \bar{v}_j}{2} - \Delta\right) \right. \\ &\quad \left. - \left(\frac{\bar{v}_i + \bar{v}_j}{2} - \Delta\right) \cos\left(\frac{\bar{v}_i + \bar{v}_j}{2} - \Delta\right) \right]. \end{aligned} \quad (30)$$

The following approximations, which will be useful later, can be inferred from the approximations above:

- $$\frac{\sin(\bar{v}_i + \Delta) + \sin(\bar{v}_j + \Delta)}{2} \approx \sin\left(\frac{\bar{v}_i + \bar{v}_j}{2} + \Delta\right) \quad (31)$$

- $$\frac{\sin(\bar{v}_i - \Delta) + \sin(\bar{v}_j - \Delta)}{2} \approx \sin\left(\frac{\bar{v}_i + \bar{v}_j}{2} - \Delta\right) \quad (32)$$

- $$\pi(\sin(\bar{v}_i + \Delta) - \sin(\bar{v}_j + \Delta)) \approx \alpha_1(\bar{v}_i - \bar{v}_j) \quad (33)$$

- $$\pi(\sin(\bar{v}_i - \Delta) - \sin(\bar{v}_j - \Delta)) \approx \alpha_2(\bar{v}_i - \bar{v}_j) \quad (34)$$

Using the approximations above, one can write $|\mathbf{p}_{UL}^i|_m - |\mathbf{p}_{UL}^j|_m|^2$ as the following:

$$\begin{aligned} & \left| |\mathbf{p}_{UL}^i|_m - |\mathbf{p}_{UL}^j|_m \right|^2 \\ & \approx \left| \int_{\pi \sin(\bar{v}_j + \Delta)}^{\pi \sin(\bar{v}_i + \Delta)} \frac{1}{2\Delta\alpha_1} \exp(j(m-1)\theta) d\theta \right. \\ & \quad \left. - \int_{\pi \sin(\bar{v}_j - \Delta)}^{\pi \sin(\bar{v}_i - \Delta)} \frac{1}{2\Delta\alpha_2} \exp(j(m-1)\theta) d\theta \right|^2 \end{aligned} \quad (35)$$

$$\begin{aligned} & = \left| \frac{1}{2\Delta} \left[\frac{\exp(j(m-1)\theta)}{j(m-1)\alpha_1} \right]_{\pi \sin(\bar{v}_j + \Delta)}^{\pi \sin(\bar{v}_i + \Delta)} \right. \\ & \quad \left. - \frac{\exp(j(m-1)\theta)}{j(m-1)\alpha_2} \right]_{\pi \sin(\bar{v}_j - \Delta)}^{\pi \sin(\bar{v}_i - \Delta)} \right|^2 \end{aligned} \quad (36)$$

$$\begin{aligned} & = \left| \frac{1}{2\Delta j(m-1)\alpha_1} \left[\exp(j(m-1)\pi \sin(\bar{v}_i + \Delta)) \right. \right. \\ & \quad \left. \left. - \exp(j(m-1)\pi \sin(\bar{v}_j + \Delta)) \right] \right. \\ & \quad \left. - \frac{1}{2\Delta j(m-1)\alpha_2} \left[\exp(j(m-1)\pi \sin(\bar{v}_i - \Delta)) \right. \right. \\ & \quad \left. \left. - \exp(j(m-1)\pi \sin(\bar{v}_j - \Delta)) \right] \right|^2 \end{aligned} \quad (37)$$

$$\begin{aligned} & = \left| \frac{\exp\left(j(m-1)\pi \frac{\sin(\bar{v}_i + \Delta) + \sin(\bar{v}_j + \Delta)}{2}\right)}{2\Delta j(m-1)\alpha_1} \right. \\ & \quad \left. 2j \sin\left((m-1)\pi \frac{\sin(\bar{v}_i + \Delta) - \sin(\bar{v}_j + \Delta)}{2}\right) \right. \\ & \quad \left. - \frac{\exp\left(j(m-1)\pi \frac{\sin(\bar{v}_i - \Delta) + \sin(\bar{v}_j - \Delta)}{2}\right)}{2\Delta j(m-1)\alpha_2} \right. \\ & \quad \left. 2j \sin\left((m-1)\pi \frac{\sin(\bar{v}_i - \Delta) - \sin(\bar{v}_j - \Delta)}{2}\right) \right|^2 \end{aligned} \quad (38)$$

$$\begin{aligned} & \approx \left| \frac{\exp\left(j(m-1)\pi \sin\left(\frac{\bar{v}_i + \bar{v}_j}{2} + \Delta\right)\right)}{2\Delta j(m-1)\alpha_1} \right. \\ & \quad \left. 2j \sin\left((m-1)\frac{\alpha_1(\bar{v}_i - \bar{v}_j)}{2}\right) \right. \\ & \quad \left. - \frac{\exp\left(j(m-1)\pi \sin\left(\frac{\bar{v}_i + \bar{v}_j}{2} - \Delta\right)\right)}{2\Delta j(m-1)\alpha_2} \right. \\ & \quad \left. 2j \sin\left((m-1)\frac{\alpha_2(\bar{v}_i - \bar{v}_j)}{2}\right) \right|^2 \end{aligned} \quad (39)$$

Note that for $\bar{v}_i - \bar{v}_j \approx 0$, by using first order Taylor expansion, we arrive at $\sin\left((m-1)\frac{\alpha_1(\bar{v}_i - \bar{v}_j)}{2}\right) \approx (m-1)\frac{\alpha_1(\bar{v}_i - \bar{v}_j)}{2}$ and $\sin\left((m-1)\frac{\alpha_2(\bar{v}_i - \bar{v}_j)}{2}\right) \approx (m-1)\frac{\alpha_2(\bar{v}_i - \bar{v}_j)}{2}$ for all $m \in \{1, \dots, M\}$. The expression in (39) can then be approximated as

$$\begin{aligned} & \approx \left| \frac{\exp\left(j(m-1)\pi \sin\left(\frac{\bar{v}_i + \bar{v}_j}{2} + \Delta\right)\right)}{2\Delta j(m-1)\alpha_1} \right. \\ & \quad \left. 2j \left((m-1)\frac{\alpha_1(\bar{v}_i - \bar{v}_j)}{2} \right) \right. \\ & \quad \left. - \frac{\exp\left(j(m-1)\pi \sin\left(\frac{\bar{v}_i + \bar{v}_j}{2} - \Delta\right)\right)}{2\Delta j(m-1)\alpha_2} \right. \\ & \quad \left. 2j \left((m-1)\frac{\alpha_2(\bar{v}_i - \bar{v}_j)}{2} \right) \right|^2 \end{aligned}$$

$$\begin{aligned}
&= \left(\frac{\bar{v}_i - \bar{v}_j}{2\Delta} \right)^2 \\
&\quad \left| \exp \left(j(m-1)\pi \sin \left(\frac{\bar{v}_i + \bar{v}_j}{2} + \Delta \right) \right) \right. \\
&\quad \left. - \exp \left(j(m-1)\pi \sin \left(\frac{\bar{v}_i + \bar{v}_j}{2} - \Delta \right) \right) \right|^2 \\
&= \left(\frac{\bar{v}_i - \bar{v}_j}{2\Delta} \right)^2 \left| \exp \left[\frac{j(m-1)\pi}{2} \left(\sin \left(\frac{\bar{v}_i + \bar{v}_j}{2} + \Delta \right) \right. \right. \right. \\
&\quad \left. \left. \left. + \sin \left(\frac{\bar{v}_i + \bar{v}_j}{2} - \Delta \right) \right) \right] \right. \\
&\quad \left. 2j \sin \left[\frac{(m-1)\pi}{2} \left(\sin \left(\frac{\bar{v}_i + \bar{v}_j}{2} + \Delta \right) \right. \right. \right. \\
&\quad \left. \left. \left. - \sin \left(\frac{\bar{v}_i + \bar{v}_j}{2} - \Delta \right) \right) \right] \right|^2
\end{aligned}$$

$$\begin{aligned}
&= \left(\frac{\bar{v}_i - \bar{v}_j}{2\Delta} \right)^2 \\
&\quad \left[2 \sin \left(\frac{(m-1)\pi}{2} \left(\sin \left(\frac{\bar{v}_i + \bar{v}_j}{2} + \Delta \right) \right. \right. \right. \\
&\quad \left. \left. \left. - \sin \left(\frac{\bar{v}_i + \bar{v}_j}{2} - \Delta \right) \right) \right) \right]^2 \\
&= \left(\frac{\bar{v}_i - \bar{v}_j}{\Delta} \right)^2 \left[\sin \left(\frac{(m-1)\pi}{2} \right. \right. \\
&\quad \left. \left. \left(\sin \left(\frac{\bar{v}_i + \bar{v}_j}{2} + \Delta \right) - \sin \left(\frac{\bar{v}_i + \bar{v}_j}{2} - \Delta \right) \right) \right) \right]^2.
\end{aligned}$$

Let us define $\Delta_{\sin} := \sin \left(\frac{\bar{v}_i + \bar{v}_j}{2} + \Delta \right) - \sin \left(\frac{\bar{v}_i + \bar{v}_j}{2} - \Delta \right)$. Then, one can write

$$\begin{aligned}
\|\mathbf{p}_{UL}^i - \mathbf{p}_{UL}^j\|^2 &= \sum_{m=1}^M |[\mathbf{p}_{UL}^i]_m - [\mathbf{p}_{UL}^j]_m|^2 \\
&\approx \left(\frac{\bar{v}_i - \bar{v}_j}{\Delta} \right)^2 \sum_{m=1}^M \left(\sin \left((m-1)\pi \frac{\Delta_{\sin}}{2} \right) \right)^2. \quad (40)
\end{aligned}$$

Similarly, one can approximate $\|\mathbf{p}_{DL}^i - \mathbf{p}_{DL}^j\|^2$ as the following:

$$\begin{aligned}
\|\mathbf{p}_{DL}^i - \mathbf{p}_{DL}^j\|^2 &= \sum_{m=1}^M |[\mathbf{p}_{DL}^i]_m - [\mathbf{p}_{DL}^j]_m|^2 \\
&\approx \left(\frac{\bar{v}_i - \bar{v}_j}{\Delta} \right)^2 \sum_{m=1}^M \left(\sin \left(f_r(m-1)\pi \frac{\Delta_{\sin}}{2} \right) \right)^2, \quad (41)
\end{aligned}$$

where $f_r := \frac{f_{DL}}{f_{UL}}$ is the ratio between the DL and UL carrier frequencies. We have

$$\begin{aligned}
&\frac{\|\mathbf{p}_{DL}^i - \mathbf{p}_{DL}^j\|^2}{\|\mathbf{p}_{UL}^i - \mathbf{p}_{UL}^j\|^2} \\
&\approx \frac{\left(\frac{\bar{v}_i - \bar{v}_j}{\Delta} \right)^2 \sum_{m=1}^M \left(\sin \left(f_r(m-1)\pi \frac{\Delta_{\sin}}{2} \right) \right)^2}{\left(\frac{\bar{v}_i - \bar{v}_j}{\Delta} \right)^2 \sum_{m=1}^M \left(\sin \left((m-1)\pi \frac{\Delta_{\sin}}{2} \right) \right)^2} \\
&= \frac{\sum_{m=1}^M \left(\sin \left(f_r(m-1)\pi \frac{\Delta_{\sin}}{2} \right) \right)^2}{\sum_{m=1}^M \left(\sin \left((m-1)\pi \frac{\Delta_{\sin}}{2} \right) \right)^2}, \quad (42)
\end{aligned}$$

where

$$\begin{aligned}
\Delta_{\sin} &= \sin \left(\frac{\bar{v}_i + \bar{v}_j}{2} + \Delta \right) - \sin \left(\frac{\bar{v}_i + \bar{v}_j}{2} - \Delta \right) \\
&= 2 \cos \left(\frac{\bar{v}_i + \bar{v}_j}{2} \right) \sin(\Delta). \quad (43)
\end{aligned}$$

Let $C := \cos \left(\frac{\bar{v}_i + \bar{v}_j}{2} \right)$ and $b := C \sin(\Delta)$. Then, Δ_{\sin} can be written as

$$\begin{aligned}
\Delta_{\sin} &= \sin \left(\frac{\bar{v}_i + \bar{v}_j}{2} + \Delta \right) - \sin \left(\frac{\bar{v}_i + \bar{v}_j}{2} - \Delta \right) \\
&= 2 \cos \left(\frac{\bar{v}_i + \bar{v}_j}{2} \right) \sin(\Delta) = 2b. \quad (44)
\end{aligned}$$

Thus, using equations (42), (43) and (44), one can write

$$\frac{\|\mathbf{p}_{DL}^i - \mathbf{p}_{DL}^j\|^2}{\|\mathbf{p}_{UL}^i - \mathbf{p}_{UL}^j\|^2} \approx \frac{\sum_{m=1}^M \left(\sin \left(f_r(m-1)\pi b \right) \right)^2}{\sum_{m=1}^M \left(\sin \left((m-1)\pi b \right) \right)^2}. \quad (45)$$

Let us denote the sine ratio as $R_{\sin} := \frac{\sum_{m=1}^M \left(\sin \left(f_r(m-1)\pi b \right) \right)^2}{\sum_{m=1}^M \left(\sin \left((m-1)\pi b \right) \right)^2}$. The K constant introduced in Lemma 1 can then be defined as the maximum value that R_{\sin} can take. \square

APPENDIX B
PROOF OF THEOREM 1

$$\begin{aligned}
& \|f(\mathbf{r}_{UL}^{test}) - \mathbf{r}_{DL}^{test}\| = \\
& \left\| f(\mathbf{r}_{UL}^{test}) - \frac{1}{|A^{UL}|} \sum_{\mathbf{r}_{UL}^i \in A^{UL}} f(\mathbf{r}_{UL}^i) \right. \\
& \quad \left. + \frac{1}{|A^{UL}|} \sum_{\mathbf{r}_{UL}^i \in A^{UL}} f(\mathbf{r}_{UL}^i) - \mathbf{r}_{DL}^{test} \right\| \\
& \leq \left\| f(\mathbf{r}_{UL}^{test}) - \frac{1}{|A^{UL}|} \sum_{\mathbf{r}_{UL}^i \in A^{UL}} f(\mathbf{r}_{UL}^i) \right\| \\
& \quad + \left\| \mathbf{r}_{DL}^{test} - \frac{1}{|A^{UL}|} \sum_{\mathbf{r}_{UL}^i \in A^{UL}} f(\mathbf{r}_{UL}^i) \right\| \\
& = \left\| f(\mathbf{r}_{UL}^{test}) - \frac{1}{|A^{UL}|} \sum_{\mathbf{r}_{UL}^i \in A^{UL}} f(\mathbf{r}_{UL}^i) \right\| \\
& \quad + \left\| \mathbf{r}_{DL}^{test} - \frac{1}{|A^{UL}|} \sum_{i: \mathbf{r}_{UL}^i \in A^{UL}} \mathbf{r}_{DL}^i \right\| \\
& + \left\| \frac{1}{|A^{UL}|} \sum_{i: \mathbf{r}_{UL}^i \in A^{UL}} \mathbf{r}_{DL}^i - \frac{1}{|A^{UL}|} \sum_{\mathbf{r}_{UL}^i \in A^{UL}} f(\mathbf{r}_{UL}^i) \right\| \\
& \leq \left\| f(\mathbf{r}_{UL}^{test}) - \frac{1}{|A^{UL}|} \sum_{\mathbf{r}_{UL}^i \in A^{UL}} f(\mathbf{r}_{UL}^i) \right\| \\
& \quad + \left\| \mathbf{r}_{DL}^{test} - \frac{1}{|A^{UL}|} \sum_{i: \mathbf{r}_{UL}^i \in A^{UL}} \mathbf{r}_{DL}^i \right\| \\
& + \left\| \frac{1}{|A^{UL}|} \sum_{i: \mathbf{r}_{UL}^i \in A^{UL}} \mathbf{r}_{DL}^i - \frac{1}{|A^{UL}|} \sum_{\mathbf{r}_{UL}^i \in A^{UL}} f(\mathbf{r}_{UL}^i) \right\| \\
& \leq \left\| f(\mathbf{r}_{UL}^{test}) - \frac{1}{|A^{UL}|} \sum_{\mathbf{r}_{UL}^i \in A^{UL}} f(\mathbf{r}_{UL}^i) \right\| \\
& \quad + \left\| \mathbf{r}_{DL}^{test} - \frac{1}{|A^{UL}|} \sum_{i: \mathbf{r}_{UL}^i \in A^{UL}} \mathbf{r}_{DL}^i \right\| \\
& \quad + \left\| \frac{1}{|A^{UL}|} \sum_{i: \mathbf{r}_{UL}^i \in A^{UL}} \|\mathbf{r}_{DL}^i - f(\mathbf{r}_{UL}^i)\| \right\|
\end{aligned}$$

Let us name $\left\| f(\mathbf{r}_{UL}^{test}) - \frac{1}{|A^{UL}|} \sum_{\mathbf{r}_{UL}^i \in A^{UL}} f(\mathbf{r}_{UL}^i) \right\|$ as (UB-1), $\left\| \mathbf{r}_{DL}^{test} - \frac{1}{|A^{UL}|} \sum_{i: \mathbf{r}_{UL}^i \in A^{UL}} \mathbf{r}_{DL}^i \right\|$ as (UB-2) and $\left\| \frac{1}{|A^{UL}|} \sum_{i: \mathbf{r}_{UL}^i \in A^{UL}} \|\mathbf{r}_{DL}^i - f(\mathbf{r}_{UL}^i)\| \right\|$ as (UB-3).

(UB-1) can be upper bounded by using Lemma 2, which is the adaptation of Lemma 1 in [34] to our study. The proof of Lemma 2 is presented in Appendix C.

Lemma 2. *Let the training sample set contain at least N training samples $\{\mathbf{r}_{UL}^i\}_{i=1}^N$ with $\mathbf{r}_{UL}^i \sim v$. Assume that the*

interpolation function $f: \mathbb{R}^{1 \times 2M-1} \rightarrow \mathbb{R}^{1 \times 2M-1}$ is Lipschitz continuous with constant L .

Let \mathbf{r}_{UL}^{test} be a test sample drawn from v independently of the training samples. Let A^{UL} be defined as in (4).

Then, for any $\epsilon > 0$, for some $\frac{1}{N\eta_\delta} \leq a < 1$ and $\delta > 0$, with probability at least

$$\begin{aligned}
& (1 - \exp(-2N((1-a)\eta_\delta)^2)) \\
& \quad \left(1 - 2\sqrt{2M-1} \exp\left(-\frac{aN\eta_\delta\epsilon^2}{2L^2\delta^2}\right)\right),
\end{aligned}$$

the set A^{UL} contains at least $aN\eta_\delta$ samples and the distance between the embedding of \mathbf{r}_{UL}^{test} and the sample mean of the embeddings of its neighboring training samples is bounded as

$$\begin{aligned}
& \left\| f(\mathbf{r}_{UL}^{test}) - \frac{1}{|A^{UL}|} \sum_{\mathbf{r}_{UL}^i \in A^{UL}} f(\mathbf{r}_{UL}^i) \right\| \\
& \leq L\delta + \sqrt{2M-1}\epsilon. \quad (46)
\end{aligned}$$

Next, (UB-2) can be bounded by using Lemma 1 as follows:

$$\begin{aligned}
& \left\| \mathbf{r}_{DL}^{test} - \frac{1}{|A^{UL}|} \sum_{\mathbf{r}_{UL}^i \in A^{UL}} \mathbf{r}_{DL}^i \right\| \\
& = \left\| \frac{1}{|A^{UL}|} \sum_{i: \mathbf{r}_{UL}^i \in A^{UL}} (\mathbf{r}_{DL}^{test} - \mathbf{r}_{DL}^i) \right\| \\
& \leq \frac{1}{|A^{UL}|} \sum_{i: \mathbf{r}_{UL}^i \in A^{UL}} \|\mathbf{r}_{DL}^{test} - \mathbf{r}_{DL}^i\| \\
& \leq \frac{1}{|A^{UL}|} \sum_{\mathbf{r}_{UL}^i \in A^{UL}} K \|\mathbf{r}_{UL}^{test} - \mathbf{r}_{UL}^i\| \\
& \leq \frac{1}{|A^{UL}|} |A^{UL}| K \delta = K\delta, \quad (47)
\end{aligned}$$

for some constant $K > 0$.

Finally, (UB-3) is the average training error of the points in A^{UL} . Thus, by finding upper bounds on (UB-1) and (UB-2) as in (46) and (47) respectively, the difference between the test error of any point and the average training error of its neighboring training points can be upper bounded as given in Theorem 1. \square

APPENDIX C
PROOF OF LEMMA 2

A training sample \mathbf{r}_{UL}^i drawn independently from \mathbf{r}_{UL}^{test} lies in a δ -neighborhood of \mathbf{r}_{UL}^{test} with probability

$$P(\mathbf{r}_{UL}^i \in B_\delta(\mathbf{r}_{UL}^{test})) = v(B_\delta(\mathbf{r}_{UL}^{test})) \geq \eta_\delta.$$

From [34] and the references therein, one can show that

$$P(|A^{UL}| \geq Q) \geq 1 - \exp\left(-\frac{2(N\eta_\delta - Q)^2}{N}\right),$$

for $1 \leq Q < N\eta_\delta$. Assuming that $|A^{UL}| \geq Q$, from [34] and the references therein, one can show that, with probability at least

$$1 - 2\sqrt{2M-1} \exp\left(-\frac{|A^{UL}| \epsilon^2}{2L^2\delta^2}\right) \geq 1 - 2\sqrt{2M-1} \exp\left(-\frac{Q\epsilon^2}{2L^2\delta^2}\right),$$

the distance between the embedding of \mathbf{r}_{UL}^{test} and the sample average of the embeddings of training samples lying inside the δ -neighborhood of \mathbf{r}_{UL}^{test} is bounded as

$$\left\| f(\mathbf{r}_{UL}^{test}) - \frac{1}{|A^{UL}|} \sum_{\mathbf{r}_{UL}^i \in A^{UL}} f(\mathbf{r}_{UL}^i) \right\| \leq L\delta + \sqrt{2M-1}\epsilon. \quad (48)$$

Let B_1 be the event that the inequality in (48) holds. Combining the probability expressions above,

$$P(|A^{UL}| \geq Q) \cap B_1 = P(|A^{UL}| \geq Q) P(B_1 | (|A^{UL}| \geq Q)) \geq \left(1 - \exp\left(-\frac{2(N\eta_\delta - Q)^2}{N}\right)\right) \left(1 - 2\sqrt{2M-1} \exp\left(-\frac{Q\epsilon^2}{2L^2\delta^2}\right)\right). \quad (49)$$

Thus, one can see that with probability at least

$$\left(1 - \exp\left(-\frac{2(N\eta_\delta - Q)^2}{N}\right)\right) \left(1 - 2\sqrt{2M-1} \exp\left(-\frac{Q\epsilon^2}{2L^2\delta^2}\right)\right),$$

$|A^{UL}| \geq Q$ and B_1 occurs. Setting $Q = aN\eta_\delta$ for $0 < a < 1$, one can reach the statement given in Lemma 2. \square

APPENDIX D

NUMERICAL ANALYSIS ABOUT THE CONSTANT K :

Since $-1 \leq C \leq 1$, we have $-\sin(\Delta) \leq b \leq \sin(\Delta)$. Since $\sin^2(\cdot)$ is an even function, it is enough to examine only the positive side of the interval, i.e., $0 \leq b \leq \sin(\Delta)$. We evaluate the K constant for different Δ values (hence, different maximum values of b) for a range of base station antenna numbers, M .

Table IV reports the values that K takes for $2 \leq M \leq 1000$ and for different Δ values, where $f_r = 1.0974$ is taken as in our communication scenario.

REFERENCES

[1] E. Björnson, J. Hoydis, L. Sanguinetti, *et al.*, “Massive mimo networks: Spectral, energy, and hardware efficiency,” *Foundations and Trends® in Signal Processing*, vol. 11, no. 3-4, pp. 154–655, 2017.
 [2] F. Rusek, D. Persson, B. K. Lau, E. G. Larsson, T. L. Marzetta, O. Edfors, and F. Tufvesson, “Scaling up mimo: Opportunities and challenges with very large arrays,” *IEEE signal processing magazine*, vol. 30, no. 1, pp. 40–60, 2012.

TABLE IV
K VALUES FOR $f_r = 1.0974$ AND FOR DIFFERENT Δ VALUES

$\Delta(^{\circ})$	Corresponding K Value
5	1.0974
10	1.0974
15	1.0974
35	1.0974
45	1.1317
60	1.1893

[3] E. Björnson, E. G. Larsson, and T. L. Marzetta, “Massive mimo: Ten myths and one critical question,” *IEEE Communications Magazine*, vol. 54, no. 2, pp. 114–123, 2016.
 [4] Y. Xu, G. Yue, and S. Mao, “User grouping for massive mimo in fdd systems: New design methods and analysis,” *IEEE Access*, vol. 2, pp. 947–959, 2014.
 [5] E. Björnson, J. Hoydis, M. Kountouris, and M. Debbah, “Massive mimo systems with non-ideal hardware: Energy efficiency, estimation, and capacity limits,” *IEEE Transactions on information theory*, vol. 60, no. 11, pp. 7112–7139, 2014.
 [6] Z. Zhong, L. Fan, and S. Ge, “Fdd massive mimo uplink and downlink channel reciprocity properties: Full or partial reciprocity?,” in *GLOBECOM 2020-2020 IEEE Global Communications Conference*, pp. 1–5, IEEE, 2020.
 [7] H. Xie, F. Gao, S. Jin, J. Fang, and Y.-C. Liang, “Channel estimation for tdd/fdd massive mimo systems with channel covariance computing,” *IEEE Transactions on Wireless Communications*, vol. 17, no. 6, pp. 4206–4218, 2018.
 [8] Y.-C. Liang and F. P. S. Chin, “Downlink channel covariance matrix (dccm) estimation and its applications in wireless ds-cdma systems,” *IEEE Journal on Selected Areas in Communications*, vol. 19, no. 2, pp. 222–232, 2001.
 [9] M. Jordan, A. Dimofte, X. Gong, and G. Ascheid, “Conversion from uplink to downlink spatio-temporal correlation with cubic splines,” in *VTC Spring 2009-IEEE 69th Vehicular Technology Conference*, pp. 1–5, IEEE, 2009.
 [10] A. Decurninge, M. Guillaud, and D. T. Slock, “Channel covariance estimation in massive mimo frequency division duplex systems,” in *2015 IEEE Globecom Workshops (GC Wkshps)*, pp. 1–6, IEEE, 2015.
 [11] M. B. Khalilsarai, S. Haghghatshoar, X. Yi, and G. Caire, “Fdd massive mimo via ul/dl channel covariance extrapolation and active channel sparsification,” *IEEE Transactions on Wireless Communications*, vol. 18, no. 1, pp. 121–135, 2018.
 [12] L. Miretti, R. L. G. Cavalcante, and S. Stańczak, “Channel covariance conversion and modelling using infinite dimensional hilbert spaces,” *IEEE Transactions on Signal Processing*, vol. 69, pp. 3145–3159, 2021.
 [13] B. Banerjee, R. C. Elliott, W. A. Krzymieñ, and H. Farmanbar, “Downlink channel estimation for fdd massive mimo using conditional generative adversarial networks,” *IEEE Transactions on Wireless Communications*, vol. 22, no. 1, pp. 122–137, 2022.
 [14] S. Bameri, K. A. Almahrog, R. H. Gohary, A. El-Keyi, and Y. A. E. Ahmed, “Uplink to downlink channel covariance transformation in fdd systems,” *IEEE Transactions on Signal Processing*, vol. 71, pp. 3196–3212, 2023.
 [15] K. Hugl, K. Kalliola, J. Laurila, *et al.*, “Spatial reciprocity of uplink and downlink radio channels in fdd systems,” in *Proc. COST*, vol. 273, p. 066, Citeseer, 2002.
 [16] C. Örnek and E. Vural, “Nonlinear supervised dimensionality reduction via smooth regular embeddings,” *Pattern Recognition*, vol. 87, pp. 55–66, 2019.
 [17] Y. Yang, F. Gao, G. Y. Li, and M. Jian, “Deep learning-based downlink channel prediction for fdd massive mimo system,” *IEEE Communications Letters*, vol. 23, no. 11, pp. 1994–1998, 2019.
 [18] W. Utschick, V. Rizzello, M. Joham, Z. Ma, and L. Piazzi, “Learning the csi recovery in fdd systems,” *IEEE Transactions on Wireless Communications*, vol. 21, no. 8, pp. 6495–6507, 2022.
 [19] J. Zeng, J. Sun, G. Gui, B. Adebisi, T. Ohtsuki, H. Gacanin, and H. Sari, “Downlink csi feedback algorithm with deep transfer learning for fdd massive mimo systems,” *IEEE Transactions on Cognitive Communications and Networking*, vol. 7, no. 4, pp. 1253–1265, 2021.
 [20] J. Wang, G. Gui, T. Ohtsuki, B. Adebisi, H. Gacanin, and H. Sari, “Compressive sampled csi feedback method based on deep learning for

- fdd massive mimo systems,” *IEEE Transactions on Communications*, vol. 69, no. 9, pp. 5873–5885, 2021.
- [21] M. Nerini, V. Rizzello, M. Joham, W. Utschick, and B. Clerckx, “Machine learning-based csi feedback with variable length in fdd massive mimo,” *IEEE Transactions on Wireless Communications*, vol. 22, no. 5, pp. 2886–2900, 2022.
- [22] A. Adhikary, J. Nam, J.-Y. Ahn, and G. Caire, “Joint spatial division and multiplexing—the large-scale array regime,” *IEEE transactions on information theory*, vol. 59, no. 10, pp. 6441–6463, 2013.
- [23] F. Sohrabi, K. M. Attiah, and W. Yu, “Deep learning for distributed channel feedback and multiuser precoding in fdd massive mimo,” *IEEE Transactions on Wireless Communications*, vol. 20, no. 7, pp. 4044–4057, 2021.
- [24] K. Li, Y. Li, L. Cheng, Q. Shi, and Z.-Q. Luo, “Downlink channel covariance matrix reconstruction for fdd massive mimo systems with limited feedback,” *IEEE Transactions on Signal Processing*, 2024.
- [25] Y. Liu and O. Simeone, “Learning how to transfer from uplink to downlink via hyper-recurrent neural network for fdd massive mimo,” *IEEE Transactions on Wireless Communications*, vol. 21, no. 10, pp. 7975–7989, 2022.
- [26] L. Miretti, R. L. G. Cavalcante, and S. Stanczak, “Fdd massive mimo channel spatial covariance conversion using projection methods,” in *2018 IEEE International Conference on Acoustics, Speech and Signal Processing (ICASSP)*, pp. 3609–3613, IEEE, 2018.
- [27] P. Isola, J.-Y. Zhu, T. Zhou, and A. A. Efros, “Image-to-image translation with conditional adversarial networks,” in *Proceedings of the IEEE conference on computer vision and pattern recognition*, pp. 1125–1134, 2017.
- [28] C. Piret, *Analytical and numerical advances in radial basis functions*. PhD thesis, University of Colorado at Boulder, 2007.
- [29] M. Belkin and P. Niyogi, “Laplacian eigenmaps for dimensionality reduction and data representation,” *Neural computation*, vol. 15, no. 6, pp. 1373–1396, 2003.
- [30] G. Roussos and B. J. Baxter, “Rapid evaluation of radial basis functions,” *Journal of Computational and Applied Mathematics*, vol. 180, no. 1, pp. 51–70, 2005.
- [31] “LTE; Evolved Universal Terrestrial Radio Access (E-UTRA); User Equipment (UE) Radio Transmission and Reception (3GPP TS 36.101 Version 14.3.0 Release 14), document ETSI TS 136 101 V14.3.0,” Apr 2017.
- [32] M. Herdin and E. Bonek, *A MIMO correlation matrix based metric for characterizing non-stationarity*. na, 2004.
- [33] K. M. Grigoriadis, A. E. Frazho, and R. E. Skelton, “Application of alternating convex projection methods for computation of positive toeplitz matrices,” *IEEE transactions on signal processing*, vol. 42, no. 7, pp. 1873–1875, 1994.
- [34] S. Kaya and E. Vural, “Learning multi-modal nonlinear embeddings: Performance bounds and an algorithm,” *CoRR*, vol. abs/2006.02330, 2020.